Pis'ma v ZhETF, vol. 93, iss. 7, pp. 408 – 413 © 2011 April 10

Second Harmonic Generation in Graphene

M. M. Glazov[1)]

Ioffe Physical-Technical Institute RAS, 194021 St. Petersburg, Russia

Submitted 25 January 2011

We report on theoretical study of second harmonic generation in graphene. Phenomenological analysis based on symmetry arguments is carried out. It is demontrated, that in ideal graphene samples second harmonic generation is possible only if the radiation wave vector or its magnetic field is taken into account. Microscopic theory is developed for the classical regime of radiation interaction with electrons, where photon energy is much smaller than the charge carriers characteristic energy. It is demonstrated, that the emitted radiation can be strongly circularly polarized for the linearly polarized incident wave.

Introduction. Graphene, a monolayer of carbon atoms arranged in honeycomb lattice, became recently one of the most promising materials owing to its intriguing electronic and transport properties, for recent reviews see Refs. [1–5] and references wherein. It is well known that *non-linear* transport and optical phenomena are most sensitive to the fine details of energy spectrum and carrier scattering in condensed matter [6, 7]. One of the non-linear effects is the generation of *dc* current under homogeneous excitation caused by the asymmetry of optical transitions and scattering in non-centrosymmetric media (photogalvanic effect) or by the transfer of photon momentum to the electron system (photon drag effect) [8]. The latter one does not require low symmetry of the structure, but it is masked by various photogalvanic effects in ordinary semiconductor quantum wells which lack an inversion center as a rule [9]. By contrast, graphene is a centrosymmetric material which allowed unambiguous identification of the photon drag effect by its remarkable polarization dependence [10].

Here we consider theoretically light wave vector induced *second harmonic generation* in graphene which consists in the formation of the *ac* response: electric current or dielectric polarization oscillating at the double frequency as compared with the frequency of the incident radiation. Experimentally second harmonic in graphene was observed in [11, 12], but microscopic theory is absent so far. Alike the photon drag effect, in centrosymmetric media like graphene second harmonic generation is allowed only provided that the photon momentum transfer to electron system is taken into account. This is in contrast to the third (and other odd) harmonic generation [13, 14] as well as coherent injection of ballistic currents [15, 16] which do not require photon momentum transfer, but appear in higher orders in incident electromagnetic field.

The second harmonic response is calculated here for low frequencies, e.g. terahertz radiation. In such case, the photon energy is much smaller than characteristic energy of electrons and a classical regime is realized for the radiation interaction with electrons in graphene, which brings about very strong polarization effects. In particular, second harmonic can be strongly circularly polarized for linearly polarized incident radiation.

Phenomenological theory. We consider an ideal single layer graphene described by the point symmetry group $D_{6\mathrm{h}}$. This point group contains an inversion center, therefore, the second harmonic generation is possible only if one takes into consideration the light wave vector $\mathbf{q}$ transfer to electron ensemble or joint action of electric $\mathbf{E}$ and magnetic fields $\mathbf{B}$ of the incident radiation [7, 8]. Since the magnetic field components B_α are proportional to certain combinations $q_\beta E_\gamma$, where greek subscripts enumerate Cartesian coordinates, in phenomenological considerations it is enough to allow for the contributions to the second order response being linear in the wave vector components and quadratic in the electric field amplitudes.

It is convenient to study the electric current, $\mathbf{j}(2\omega)$, induced at the double frequency 2ω as a response to the incident radiation with the fundamental frequency ω. The electric current is related with the oscillating polarization, $\mathbf{P}(2\omega)$, as $\mathbf{j}(2\omega) = -2\mathrm{i}\omega\mathbf{P}(2\omega)$. The general phenomenological expression describing the second harmonic generation reads

$$j_\lambda(2\omega) = S_{\lambda\mu\nu\eta} q_\mu E_\nu E_\eta. \quad (1)$$

Here $S_{\lambda\mu\nu\eta}$ is the material tensor and the electric field of the fundamental wave is taken in the complex form

$$\mathbf{E}(\mathbf{r},t) = \mathbf{E}e^{\mathrm{i}(\mathbf{qr}-\omega t)} + \mathrm{c.c.} \quad (2)$$

[1)]e-mail: glazov@coherent.ioffe.ru

The same complex form, Eq. (2), is assumed for all other quantities in question: the magnetic field, $\mathbf{B}$, and the current density, $\mathbf{j}$. It is worth mentioning that, in contrast to the photon drag effect where the *dc* current is proportional to the bilinear combinations of electric field and its conjugate, $E_\nu E_\eta^*$, the second harmonic generation is described by the quadratic combinations $E_\nu E_\eta$. Hence, tensor $S_{\lambda\mu\nu\eta}$ is invariant with respect to permutations of the two last subscripts. The elements $S_{\lambda\mu\nu\eta}$ are, in general, complex, the presence of both real and imaginary parts describes the phase shift between the fundamental and second harmonics.

There are 7 independent parameters, $S_1 \dots S_7$, which describe second harmonic generation in the system of point group $D_{6\mathrm{h}}$:

$$j_x(2\omega) = S_1 q_x(E_x^2+E_y^2)+S_2[q_x(E_x^2-E_y^2)+2q_yE_xE_y] + S_3q_zE_xE_z + S_4q_xE_z^2, \quad (3a)$$

$$j_y(2\omega) = S_1 q_y(E_x^2+E_y^2)+S_2[q_y(E_y^2-E_x^2)+2q_xE_xE_y] + S_3q_zE_yE_z + S_4q_yE_z^2, \quad (3b)$$

$$j_z(2\omega) = S_5q_zE_z^2 + S_6q_z(E_x^2+E_y^2) + + S_7(q_xE_xE_z + q_yE_yE_z), \quad (3c)$$

where we assumed that the graphene layer occupies (xy) plane. Expressions (3a) and (3b) are similar to phenomenological equations describing linear drag effect in graphene [17].

The specifics of the graphene band structure imposes strong restrictions on values of the constants $S_1, \dots, S_7$ in Eqs. (3). Indeed, conduction and valence bands of graphene are formed from π orbitals of carbon atoms. As a result, the transitions in z polarization are possible only with allowance for other, σ, orbitals which are separated from π orbitals by several electronvolts. It implies that in the model where only π orbitals are taken into account (e.g. in the classical frequency range of interest) constants $S_i = 0$ for $i > 2$ and second harmonic generation is described by the simplified expressions with only two independent parameters:

$$j_x(2\omega)=S_1q_x(E_x^2+E_y^2)+S_2[q_x(E_x^2-E_y^2)+2q_yE_xE_y], \quad (4a)$$

$$j_y(2\omega)=S_1q_y(E_x^2+E_y^2)+S_2[q_y(E_y^2-E_x^2)+2q_xE_xE_y]. \quad (4b)$$

Figure 1 schematically shows the geometry of the second harmonic generation and the response at a double frequency, 2ω. For instance, for $q_x \neq 0$, $q_y = 0$, there is a component of the in-plane oscillating current $\mathbf{j}(2\omega)$ parallel to the light incidence plane described by $(S_1+S_2)q_xE_x^2 + (S_1-S_2)q_xE_y^2$ (Fig. 1a). Additionally, there is a transverse contribution, $2S_2q_xE_xE_y$, Fig. 1b. Microscopic theory for these constants S_1 and S_2 is developed below.

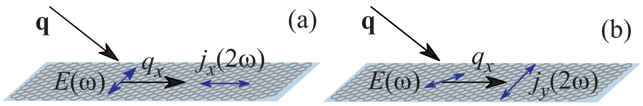

Fig. 1. Schematic illustration of the second harmonic generation geometry, Eqs. (4). It is seen that there are both longitudinal [panel (a)] and transverse [panel (b)] components of the second order response

Graphene samples are usually deposited on substrates, hence $z \to -z$ symmetry is broken. As a result, structure becomes non-centrosymmetric, described by the point group $C_{6\mathrm{v}}$, and second harmonic generation becomes possible for $\mathbf{q} = 0$. It can be shown that additional contributions have the following form

$$j_x(2\omega) = S_3'E_xE_z, \quad j_y(2\omega) = S_3'E_yE_z, \quad (5a)$$

$$j_z(2\omega) = S_5'E_z^2 + S_6'(E_x^2+E_y^2), \quad (5b)$$

where S_3', S_5' and S_6' are some coefficients directly proportional to parameters ∂_{15}^t, ∂_{31}^t and ∂_{33}^t introduced in Eq. (10) of Ref. [12]. As one can see from Eqs. (5) these contributions require transitions in z polarization and are strongly suppressed in classical frequency range [17] but they may take over for higher frequencies [12].

Microscopic theory. We consider here a doped graphene layer and assume that the characteristic electron energy (being the Fermi energy, ε_F, for degenerate and the temperature, $k_\mathrm{B}T$, for non-degenerate electrons) is much larger than the photon energy $\hbar\omega$. This condition allows one to treat electron dynamics in the framework of Boltzmann equation. For typical carrier densities on the order of 10^{12} cm^{-2} the electron Fermi energy $\varepsilon_\mathrm{F} \sim 100$ meV, therefore carriers are degenerate even at room temperature and classical treatment is valid for microwave or terahertz radiation [10].

We introduce time, t, position, $\mathbf{r}$, and momentum, $\mathbf{p}$, dependent electron distribution function $f(\mathbf{p},\mathbf{r},t)$ which satisfies standard kinetic equation [10, 17]

$$\frac{\partial f}{\partial t} + \mathbf{v}_\mathbf{p}\frac{\partial f}{\partial \mathbf{r}} + e\left(\mathbf{E} + \frac{1}{c}[\mathbf{v}_\mathbf{p}\times\mathbf{B}]\right)\frac{\partial f}{\partial \mathbf{p}} = Q\{f\}. \quad (6)$$

Here $\mathbf{E}$ and $\mathbf{B}$ are the electric and magnetic fields of the incident wave taken in the form Eq. (2), e is the electron charge, $e = -|e|$, c is the speed of light, $\mathbf{v_p}$ is the electron velocity in the given state $\mathbf{p}$,

$$\mathbf{v_p} = \frac{\partial \varepsilon_p}{\partial \mathbf{p}} = v\frac{\mathbf{p}}{|\mathbf{p}|}. \tag{7}$$

Here $\varepsilon_p = v|\mathbf{p}|$ is the electron dispersion, $v \approx c/300$ is effective electron speed in graphene, and $Q\{f\}$ in Eq. (6) is the collision integral. In Eq. (6) it is assumed that $f(\mathbf{p},\mathbf{r},t)$ describes the electron distribution in any of two equivalent degenerate valleys, K and K'. It is clearly seen from Eq. (6) that electron motion is affected by the in-plane components of electric field $\mathbf{E}$ and by z component of magnetic field $\mathbf{B}$.

The distribution function is sought in a form [17]

$$f(\mathbf{k},\mathbf{r},t) = f_0(\varepsilon) + [f_1^{\omega}(\mathbf{k})e^{\mathrm{i}(\mathbf{qr}-\omega t)} + \text{c.c.}] + \\ + f_2^0(\mathbf{k}) + [f_2^{2\omega}(\mathbf{k})e^{2\mathrm{i}(\mathbf{qr}-\omega t)} + \text{c.c.}], \tag{8}$$

where $f_0(\varepsilon)$ is the equilibrium (Fermi-Dirac) distribution function, $f_1^{\omega}(\mathbf{k})$ is the first order correction, and functions f_2^0, $f_2^{2\omega}$ are the second order corrections corresponding to the responses at zero frequency (photon drag effect) and at the frequency 2ω (second harmonic), respectively. The terms containing higher frequencies (and, hence, higher powers of $\mathbf{E}$, $\mathbf{B}$) are disregarded here because they do not contribute to the second harmonic generation. The *dc* response was calculated in Refs. [10, 17], below we find the function $f_2^{2\omega}(\mathbf{k})$.

In order to determine $f_2^{2\omega}(\mathbf{k})$ we solve Eq. (6) by iterations. To that end one has to find first order correction, $f_1^{\omega}(\mathbf{k})$, which can be expressed up to the linear in $\mathbf{q}$ terms as [17]

$$f_1(\mathbf{k}) = -e\tau_{1,\omega} f_0' \Bigg\{ (\mathbf{E}_0\mathbf{v_p}) - \\ - \mathrm{i}\tau_{2,\omega}[(\mathbf{qv_p})(\mathbf{E}_0\mathbf{v_p}) - v^2(\mathbf{qE}_0)/2] + \frac{v^2(\mathbf{qE}_0)}{2\omega}\Bigg\}. \tag{9}$$

Here we introduced $f_0' = \mathrm{d}f_0/\mathrm{d}\varepsilon$,

$$\tau_{n,\omega} = \frac{\tau_n}{1-\mathrm{i}\omega\tau_n} \quad (n=1,2),$$

where τ_1 and τ_2 are the relaxation times for the first and second angular harmonics of the distribution function which describe the momentum (first angular harmonic) and momentum alignment (second angular harmonic) relaxation of electrons, respectively. These relaxation times can be determined in Born approximation as [18]

$$\frac{1}{\tau_n} \equiv \frac{1}{\tau_n(\varepsilon_k)} = \\ = \frac{2\pi}{\hbar} n_{\text{imp}} \sum_{\mathbf{p}} |V_{\mathbf{k}-\mathbf{p}}|^2 \frac{1+\cos\vartheta}{2}[1-\cos(n\vartheta)]\delta(\varepsilon_k - \varepsilon_p), \tag{10}$$

where n_{imp} is the (two-dimensional) impurity density, $V_{\mathbf{q}}$ is the Fourier-transform of the impurity potential, ϑ is the scattering angle, $(1+\cos\vartheta)/2$ comes from the overlap of Bloch amplitudes and the normalization area is set to unity hereafter. Intervalley scattering processes are disregarded in Eq. (10).

The energy relaxation processes are neglected assuming that $\omega\tau_\varepsilon \gg 1$, $\tau_\varepsilon/\tau_{1,2} \gg 1$, where τ_ε is the energy relaxation time. Equation (9) is valid as long as $qv\tau_1, qv\tau_2, qv/\omega \ll 1$, that is if spatial variations of the distribution function occur on the scale exceeding by far the mean free path, this condition is readily fulfilled in the relevant frequency range.

The second order correction satisfies the following equation

$$-2\mathrm{i}\omega f_2^{2\omega}(\mathbf{p}) + 2\mathrm{i}\mathbf{qv_p} f_2^{2\omega}(\mathbf{p}) + \\ + e\left(\mathbf{E} + \tfrac{1}{c}[\mathbf{v_p}\times\mathbf{B}]\right)\tfrac{\partial f_1^{\omega}(\mathbf{p})}{\partial \mathbf{p}} = Q\{f_2^{2\omega}\}, \tag{11}$$

and the electric current density is given by:

$$\mathbf{j} = 4e\sum_{\mathbf{k}} \mathbf{v_p} f_2^{2\omega}(\mathbf{p}), \tag{12}$$

where the factor 4 takes into account spin and valley degeneracy. Solving Eq. (11), retaining in $f_2^{2\omega}(\mathbf{p})$ only linear in $\mathbf{q}$ or linear in $\mathbf{B}$ terms and expressing $\mathbf{B} = [(\mathbf{q}/q)\times\mathbf{E}]$ (for the sample in vacuum) we arrive at the following expressions for the constants S_1 and S_2:

$$S_1 = -\frac{e^3v^4}{2\omega}\sum_{\mathbf{k}} \tau_{1,\omega} f_0' \times \\ \times \left[\frac{\tau_{1,2\omega}}{\varepsilon_k}(3+\mathrm{i}\omega\tau_{2,\omega}) + (1-\mathrm{i}\omega\tau_{2,\omega})\frac{\mathrm{d}\tau_{1,2\omega}}{\mathrm{d}\varepsilon_k}\right], \tag{13a}$$

$$S_2 = \frac{e^3v^4}{2\omega}\sum_{\mathbf{k}} \tau_{1,\omega} f_0' \times \\ \times \left\{\frac{\tau_{1,2\omega}}{\varepsilon_k}(1+4\mathrm{i}\omega\tau_{2,2\omega}) - \frac{\mathrm{d}}{\mathrm{d}\varepsilon_k}[\tau_{1,2\omega}(1-2\mathrm{i}\omega\tau_{2,2\omega})]\right\}. \tag{13b}$$

It is noteworthy, that the physical mechanisms governing second harmonic generation are the same as in the photon drag effect [17]. First one is related to the joint action of electric and magnetic fields of the incident radiation: electric field induces *ac* current with the fundamental frequency ω, while magnetic field oscillating at the same frequency induces both *dc* current and the current component with the double frequency, 2ω. This is EB mechanism of the second harmonic generation. Another (qE^2) mechanism is connected with the spatial dependence of the electric field, its qualitative description can be carried out along the same lines as in Ref. [17].

In quantum language the microscopic mechanisms governing these effects are due to the magneto-dipole and quadrupole transitions, respectively.

Figure 2 shows frequency dependence of electric current components at double frequency $j(2\omega)$ proportional to coefficients S_1 [panel (a)] and S_2 [panel (b)], respectively. Calculation is carried out for the short-range scattering where $V_{\mathbf{k}-\mathbf{p}}$ in Eq. (10) is constant and relaxation times are interrelated as $\tau_1 = 2\tau_2 \propto \varepsilon_k^{-1}$. The electron gas is assumed to be degenerate. It can be seen that the response at double frequency has complex non-monotonous behavior. In the static limit, $\omega \to 0$, the coefficients S_1 and S_2 are real and diverge as $1/\omega$, but the net current remains finite due to factors $\propto \mathbf{q}$ in Eqs. (4). Coefficients S_1 and S_2 become, up to common factor, equal to the constants T_1 and T_2 describing linear photon drag effect, see Eqs. (26) of Ref. [17], because at $\omega = 0$ responses at zero and double frequencies are indistinguishable. At high frequencies, $\omega\tau_1 \gg 1$, $\omega\tau_2 \gg 1$, parameters S_1 and S_2 are proportional to $1/\omega^3$, hence, current density decays as $1/\omega^2$. The imaginary part of current is determined by the retardation between the driving electric field and electron velocity [10, 17]. Therefore, it is zero in the limit of static fields, shows maximum at $\omega\tau_1 \sim 1$ and decreases for $\omega\tau_1 \gg 1$. Typical values of $j(2\omega)$ for $\omega\tau_1 \sim 1$ are close to those of *dc* current. For the experimental parameters of Ref. [10]: $j(2\omega)/P \sim 0.5$ nAcm/W, where P is the power density.

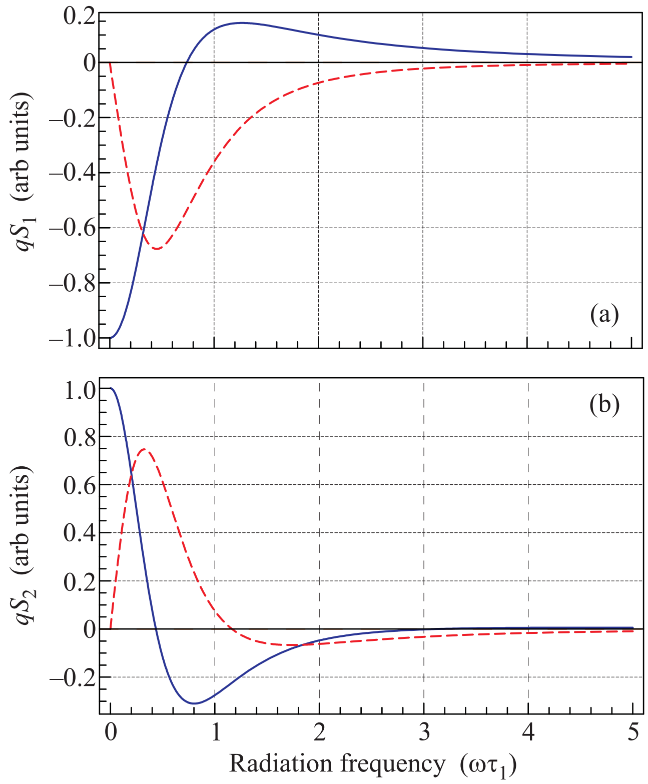

Fig. 2. Frequency dependence of the contributions to the second harmonic response: qS_1 is shown in panel (a), and qS_2 is shown in panel (b). Solid blue lines depict real part and dashed red lines depict imaginary part of the response. Values of current are given in arbitrary units, radiation frequency is presented in units of $\omega\tau_1$, where τ_1 is momentum relaxation time. Calculation is carried out for the short-range scattering where $\tau_1 = 2\tau_2 \propto \varepsilon_k^{-1}$ for degenerate electrons

Polarization of the second harmonic. The electromagnetic field emitted at the double frequency can be found by means of Maxwell equations. It is convenient to determine the vector potential $\mathbf{A}(\mathbf{r},t)$ oscillating at 2ω, which satisfies the following equation [19]

$$\Delta\mathbf{A}(\mathbf{r},t)+\frac{4\omega^2}{c^2}\mathbf{A}(2\omega)= -\frac{4\pi}{c}\mathrm{e}^{2\mathrm{i}\mathbf{q}_\parallel\boldsymbol{\rho}-2\mathrm{i}\omega t}\delta(z)\mathbf{j}(2\omega) + \text{c.c.} \tag{14}$$

where $\mathbf{q}_\parallel = (q_x, q_y)$ is the projection of the incident radiation wave vector onto the graphene layer and we assumed that the sample is positioned in vacuum at $z = 0$ plane. Using one-dimensional Green's function [8], the solution of Eq. (14) can be written as

$$\mathbf{A}(\mathbf{r},t) = \frac{\mathrm{i}\pi}{cq_z}\mathrm{e}^{2\mathrm{i}\mathbf{q}_\parallel\boldsymbol{\rho}-2\mathrm{i}\omega t}\Big[\mathbf{j}(2\omega)\mathrm{e}^{2\mathrm{i}q_z|z|} - -\mathbf{e}_z\frac{\mathbf{j}(2\omega)\mathbf{q}_\parallel}{q_z}(\mathrm{e}^{2\mathrm{i}q_z|z|}-1)\mathrm{sign}(z)\Big] + \text{c.c.} \tag{15}$$

Here $\mathbf{e}_z$ is the unit vector along z-axis. It follows from Eq. (15) that the emitted radiation propagates with the in-plane wave vector $2\mathbf{q}_\parallel$. The dependence of the vector potential on z given by the factor $\exp(2\mathrm{i}q_z|z|)$ corresponds to the wave diverging from the quantum well.

The electric field of the emitted second harmonic is related with its vector potential by the standard expression $\mathbf{E}(2\omega) = -c^{-1}\partial\mathbf{A}(2\omega)/\partial t$. Making use of Eq. (15) one can see that the Stokes parameters of emitted radiation are given by

$$\begin{aligned} P_l(2\omega) &= \frac{|j_x(2\omega)|^2 - |j_y(2\omega)|^2}{|j_x(2\omega)|^2 + |j_y(2\omega)|^2}, \\ P_l'(2\omega) &= \frac{2\mathrm{Re}\{j_x(2\omega)j_y^*(2\omega)\}}{|j_x(2\omega)|^2 + |j_y(2\omega)|^2}, \\ P_c(2\omega) &= -\frac{2\mathrm{Im}\{j_x(2\omega)j_y^*(2\omega)\}}{|j_x(2\omega)|^2 + |j_y(2\omega)|^2}. \end{aligned} \tag{16}$$

Here P_l and P_l' are the degrees of linear polarization in two coordinate frames: the xy frame and in the $x'y'$ frame which is rotated by 45° with respect to xy

frame. Quantity P_c is the circular polarization degree. In derivation of Eqs. (16) we assumed small incidence angles, $q_{\|} \ll q_z$, and considered the emitted wave propagating along positive z axis.

We assume that the in-plane wave vector is directed along x axis, $q_x \neq 0$, $q_y = 0$. Non-trivial polarization effects take place if both $j_x(2\omega)$ and $j_y(2\omega)$ are non-zero. Such situation may arise for the linearly polarized incident radiation in $x'y'$ axis frame, where $|E_x|^2 = |E_y|^2$, $2\mathrm{Re}\{E_x E_y^*\} = |E_x|^2 + |E_y|^2$ [$P_l(\omega) = 0$, $P_l'(\omega) = 1$, $P_c(\omega) = 0$] which is considered in the following. Stokes parameters for the second harmonic are plotted in Fig. 3 as functions of the fundamental radiation

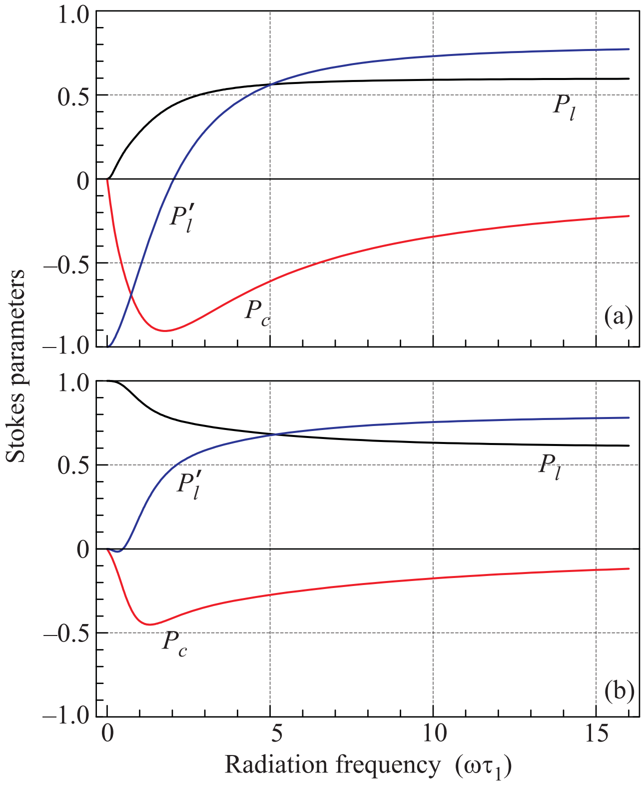

Fig. 3. Frequency dependence of Stokes parameters of second harmonic: P_l is shown by black, P_l' by blue and P_c by red curves, respectively. It is assumed that the fundamental harmonic is fully linearly polarized in $x'y'$ axis frame: $|E_x|^2 = |E_y|^2$, $2\mathrm{Re}\{E_x E_y^*\} = |E_x|^2 + |E_y|^2$. Calculation is carried out for degenerate electrons in the model of the short-range scattering where $\tau_1 = 2\tau_2 \propto \varepsilon_k^{-1}$ [panel (a)] and of the Coulomb scattering where $\tau_1 = 3\tau_2 \propto \varepsilon_k$ [panel (b)]

frequency. Calculation presented in Fig. 3a is carried out for the short-range scattering where $\tau_1 = 2\tau_2 \propto \varepsilon_k^{-1}$ [panel (a)]. For comparison Fig. 3b shows calculation results for the unscreened Coulomb scattering potential, where $V_{\mathbf{k}-\mathbf{p}} \propto |\mathbf{k}-\mathbf{p}|^{-1}$ in Eq. (10) and one can show that $\tau_1 = 3\tau_2 \propto \varepsilon_k$. In all calculations it is assumed that the electron gas is degenerate.

Figure 3 clearly demonstrates that all Stokes parameters are non-zero, in general. In the limit of static fields, $\omega\tau_1 = 0$, ellipticity is forbidden, $P_c(2\omega) = 0$ in agreement with Fig. 3. In the limit of high frequencies $\omega\tau_1, \omega\tau_2 \gg 1$ (but $\hbar\omega \ll \varepsilon_{\mathrm{F}}$) constants S_1 and S_2 are related as $S_2 = S_1/2$ which yields

$$P_l = \frac{3}{5}, \quad P_l' = \frac{4}{5}, \quad P_c = 0, \quad \text{at} \quad \omega\tau_1, \omega\tau_2 \gg 1.$$

It follows from Fig. 3 that second harmonic radiation is, in general, elliptically polarized. The remarkable degree of circular polarization appears at $\omega\tau_1 \sim 1$. For the short-range scattering considered in panel (a) of Fig. 3 the maximum absolute value of the circular polarization $|P_c|$ is about 90% at $\omega\tau_1 \approx 1.78$. The maximum value of the circular polarization degree for the Coulomb scattering is somewhat smaller, $|P_c| \approx 45\%$ at $\omega\tau_1 \approx 1.31$. Physically, the circularly polarized second harmonic emission is a result of retardation: $j_x(2\omega)$ and $j_y(2\omega)$ are phase shifted with respect to each other. This phase difference can be significant resulting in almost fully circularly polarized second harmonic emission. In agreement with qualitative considerations and Fig. 2, the phase shift vanishes both for static and high frequency fields, where S_1 and S_2 are real. Circular polarization approaches zero in these two limits.

The appearance of the linear polarization in xy axis frame, $P_l(2\omega) \neq 0$, and of the circular polarization, $P_c(2\omega) \neq 0$ can be considered as a non-linear polarization conversion process. Inversion of initial linear polarization $P_l'(\omega) \to -1$ results in the reversal of the circular polarization, P_c, and of the linear polarization in $x'y'$ axis frame, $P_l'(2\omega)$. Linear polarization in xy axis frame does not change its sign.

Concluding remarks. We have developed theory of second harmonic generation in graphene. The analysis shows that in the simplest model of conduction and valence bands formed by π orbitals of carbon atoms, the response at the double frequency appears with allowance for the photon wave vector transfer to electron system and it is described by two independent parameters. The microscopic theory is presented here for the classical frequency range, where the photon energy is much smaller than the characteristic energy of charge carriers in graphene. In this regime effects of other orbitals are negligible and the second harmonic generation is fully determined by the specifics of the radiation momentum transfer to "Dirac" electrons in graphene.

We have analyzed the polarization of the emitted radiation. It is demonstrated, that even for linearly polarized fundamental harmonic, the second harmonic can be strongly circularly polarized. The degree of circular polarization can be controlled by the radiation frequency, it can be reversed by changing the linear polarization of incident wave.

Author is grateful to E.L. Ivchenko and S.A. Tarasenko for valuable discussions. The support by RFBR and "Dynasty" Foundation–ICFPM is gratefully acknowledged.

---

1. Y. E. Lozovik, S. P. Merkulova, and A. A. Sokolik, Physics Uspekhi **51**, 727 (2008).
2. S. V. Morozov, K. S. Novoselov, and A. K. Geim, Physics Uspekhi **51**, 744, (2008).
3. L. A. Falkovsky, Physics Uspekhi **51**, 887 (2008).
4. A. H. Castro Neto, F. Guinea, N. M. R. Peres et al., Rev. Mod. Phys. **81**, 109 (2009).
5. N. M. R. Peres, Rev. Mod. Phys. **82**, 2673 (2010).
6. S. D. Ganichev and W. Prettl, *Intense Terahertz Excitation of Semiconductors*, Oxford, UK, 2006.
7. M. Fiebig, V. V. Pavlov, and R. V. Pisarev, J. Opt. Soc. Am. B **22**, 96 (2005).
8. E. L. Ivchenko, *Optical Spectroscopy of Semiconductor Nanostructures*, Alpha Science, Harrow UK, 2005.
9. E. L. Ivchenko and S. Ganichev, in *Spin physics in semiconductors*, Ed. M. I. Dyakonov, Springer-Verlag, 2008.
10. J. Karch, P. Olbrich, M. Schmalzbauer et al., Phys. Rev. Lett. **105**, 227402 (2010).
11. J. J. Dean and H. M. van Driel, Appl. Phys. Lett. **95**, 261910 (2009).
12. J. J. Dean and H. M. van Driel, Phys. Rev. B **82**, 125411 (2010).
13. F. T. Vasko, preprint arXiv:1011.4841 (2010).
14. S. A. Mikhailov and K. Ziegler, Journal of Phys.: Cond. Mat. **20**, 384204 (2008).
15. E. Hendry, P. J. Hale, J. Moger et al., Phys. Rev. Lett. **105**, 097401 (2010).
16. D. Sun, C. Divin, J. Rioux et al., Nano Letters **10**, 1293 (2010).
17. J. Karch, P. Olbrich, M. Schmalzbauer et al., preprint arXiv:1002.1047 (2010).
18. S. Das Sarma, S. Adam, E. H. Hwang, and E. Rossi, preprint arXiv:1003.4731 (2010).
19. L. D. Landau and E. M. Lifshitz, *The Classical Theory of Fields*, Butterworth-Heinemann, Oxford UK, (1975).